Using Handheld Raman Spectroscopy Equipped with Orbital Raster Technology for Field Detection of Cocaine and its Impurities in Fingernails

Megan Wilson[1 *], Jason Birkett[1], Iftikhar Khan[1], Ismail Abbas[2] and Sulaf Assi[1]

[1]School of Pharmacy and Biomolecular Sciences, Liverpool John Moores University, L3 3AF, UK.

[2]Faculty of Science, Lebanese University, Beirut, Lebanon.

*Email: m.wilson3@2019.ljmu.ac.uk

Abstract

Fingernails have shown the ability to accumulate drugs as a result of chronic exposure. Raman spectroscopy is a portable technique and provides rapid analysis of chemical substances including drugs. This work employed Raman spectroscopy for detection of cocaine hydrochloride (HCl) and its impurities within fingernails. More specifically, the work utilized a novel approach in Raman spectroscopy, that is Orbital Raster Scanning technology where the laser beam hits multiple positions within the sample. This in turns maintained sensitivity and ensured that more of each sample's components were represented. Fingernails were spiked with powder and solution forms of cocaine HCl and its impurities including benzocaine HCl, levamisole HCl, lidocaine HCl, and procaine HCl. The strong Raman scattering observed for these substances indicated a high drug accumulation in the fingernails. Upon analysis key cocaine HCl bands were seen at 848, 874 and 898 cm^{-1} (C-C stretching-tropane ring), 1004 cm^{-1} (symmetric stretching-aromatic ring), 1278 cm^{-1} (C-N stretching), 1453 cm^{-1} (asymmetric CH_3 deformation) and 1605 and 1712 cm^{-1} (C=C and C=O stretching). Principle component analysis (PCA) confirmed that 90% (nails spiked with drug powders) and 77.2% (nails spiked with drug solutions) were accounted for in the variance among the data. In conclusion, the findings showed

that Raman spectroscopy identified the presence of cocaine HCl and its impurities within fingernails.

Introduction

The pervasive use of illicit drugs in the modern civilizations is a phenomenon that has never occurred in the history of humanity (1). Around 275 million individuals have used drugs in 2021, an increase of 22% from 2010. It is estimated that projected population growth for 2030 translates into a possible rise of 11% in the percentage of drug users worldwide, with a far higher impact in low-income nations than in high-income ones. The usage of drugs has been leading to numerous severe problems (2). Drug addiction has caused young individuals to drop out of school and made it difficult for parents to care for their children. It undermines ambition, drags individuals into poverty and crime, and wrecks lives. Furthermore, the illicit drug trade hinders social and economic advancement and causes serious danger to both global security and stability in some parts of the world. Within the illegal drug market, cocaine has been one of the most common substances with an estimated 2,000 metric tons of production per year (3). Cocaine is a stimulant that exerts its mechanism of action by producing a build-up of dopamine between synapses. Three main forms of cocaine are available: free base, "crack" rocks, and hydrochloride (HCl) powder (4,5).

Many investigating authorities across the world routinely seize cocaine and take judicial actions. Forensic scientists and law enforcement organizations require rapid, accurate, and adaptable techniques of drug detection to combat drugs addiction. Despite the existence of numerous detection techniques, including immunoassays (6), capillary electrophoresis (7), DNA aptameric sensors (8), and nuclear magnetic resonance (NMR) spectroscopy (9), the so-called hyphenated methods are currently the industry standard for the analysis of such illicit drugs in the fingernails and other matrices. Of the hyphenated techniques, gas chromatography/mass spectrometry (GC-MS) and Liquid chromatography/mass spectrometry (LC-MS) are often used in these analyses (10). Both GC-MS and LC-MS are destructive, time-consuming, and involve the use chemicals that can be harmful to both the operator and the environment, despite their great sensitivity and molecular specificity. Hence, the use of vibrational techniques such as Fourier transform infrared (FTIR) (11) and Raman

spectroscopy (12) is considered as a reliable alternative as these methods offer a portable, quick, non-destructive, and cost-effective solution for drug analysis. More specifically, Raman spectroscopy is a versatile technique that is applied to analyze different types of forensic samples that cannot be determined by other spectroscopic methods such as IR (13). It is used for both qualitative and quantitative purposes (14, 15). Numerous drug classes including amfetamines, date rape drugs and designer drugs have been studied using Raman spectroscopy (16); and this is due to the nature of Raman in having better chemical specificity than IR (17). The chemical specificity offers advantages of Raman in detecting physical and chemical differences between isomers and analogues of the same drug (18). Recent developments in data analysis, portable Raman spectrometers, and new excitation wavelengths offer exciting new opportunities for Raman spectroscopy applications in the detection and quantification of drugs of abuse, including investigations carried out immediately at the crime scene. Raman spectroscopy is regarded as a Category A technology, offering the maximum level of selectivity through structural information, according to worldwide recommendations given by the Scientific Working Group on Drugs (SWGDRUG)'s Core Committee (19). An emerging technique for quick on-site detection of illicit drugs is handheld Raman spectroscopy that offers additional features over conventional Raman in safety and security where the operator does not need to touch the sample that can be measured inside original packaging (20-23). The aim of this study is to demonstrate the application of rapid, portable methods for the quantitative detection of cocaine HCl and its impurities in human fingernails using handheld Raman spectroscopy in combination with chemometrics.

Materials and Methods

This work comprised Raman spectroscopic analysis of 20 sets (11 males and nine females) of fingernails of adults of two ethnicities. Fingernail clippings of 1-2 mm were collected and measured through glass vials. No intervention was made by the researchers during the collection of the fingernail clippings, considering this procedure as an everyday activity. Ethical approval was provided from two institutions: Liverpool John Moores University in the (PBS/2021-22/04) and the Lebanese University in Lebanon (2022-0104). Five sets of fingernail clippings were then spiked with one of the following drugs or drug impurities including: benzocaine

(BEN), cocaine HCl (COC), levamisole HCl (LEV), lidocaine HCl (LID), and procaine HCl (PRO). After six-weeks of spiking, the spiked nails were measured using the handheld Metrohm Mira XTR Raman spectrometer equipped with a 785 nm laser wavelength, and < 100 mW laser output power. Raman spectra were collected over the wavenumber range of 400 – 2300 cm^{-1} with spectral resolution of 10 cm^{-1}. The laser beam of the spectrometer works by orbital raster scanning (ORS) technology where it hits multiple positions within the sample.

References samples of the chosen drugs and impurities were taken through glass vials and included in the instrumental library. The inbuilt spectral algorithm searched for matches between the reference samples and spiked fingernail clipping samples. Matches were shown for the chosen drug and its impurities and highlighted key spectral features between the drug and impurities. Offline analysis was also carried out in Matlab 2022b, whereby the spectra of the drug and impurities were interpreted based on spectral quality, functional groups and similarities among the substances identified through principal component analysis (PCA) algorithm. Spectral quality was evaluated for the measured drug and drug impurities. For PCA, the Raman spectra were investigated for patterns among their PC scores. False negatives were observed when a drug/impurity score was not grouped with the scores of the same drug/impurity, where false positives were seen when a drug/impurity score was clustered with scores of a different drug or impurity.

Results and Discussion

The measured nails consisted of 20 sets of fingernails obtained from different individuals within the age group of 18-64 years old. The male: female ratio of these individuals was (11:9), and they were of (two) ethnicities including: white British and Arab. Each nail set consisted of 7-10 fingernail clippings and the dimension of each fingernail clipping was 1-2 mm. Out of the 20 sets, five sets were spiked with: BEN, COC, LEV, LID, and PRO respectively. Two types of spiking were made: powder form of the drug (3-5 nails per set) and liquid form (3-5 nails per set). A minimum of 20 spectra were collected per each nail set (whether plain or spiked).

Raman Activity of Drugs

Raman spectroscopy was able to detect COC and its impurities in fingernails six weeks post-spiking (Figure 1). In this respect, nail samples showed strong spectral quality with maximum intensity up to 30,000 a.u.

Raman activity of the chosen drug and impurities was determined through investigating their Raman spectral quality (Table 1). In turn, Raman spectra were evaluated using the following parameters: the number of peaks (N), maximum peak position/intensity, wavenumber range and signal-to-noise ratio (S/N). In this respect, BEN powder, LID powder, and LID solution showed strong Raman activity with N, max intensity and SNR in the range of 29-45, 11-74 a.u., and 33-42 respectively. BEN liquid, COC HCl powder, LEV HCl powder, LEV HCL liquid, PRO HCl powder, PRO HCl liquid displayed a medium Raman activity with N, max intensity, and SNR in the range of 16-28, 12-66 and 20-29, respectively. COC HCl liquid showed low Raman activity with N, max intensity, and SNR as 19, 28 a.u. and 25, respectively.

Effect of Physical Form on Raman Activity

Key variations were seen in the Raman activity between drugs in solid versus liquid forms (figure 2). This in turn depended on the type of drug being analyzed as some drugs showed no difference in Raman activity in solid vs liquid forms. This was the case for LEV and PRO, which both showed a medium Raman activity in their solid and liquid forms. LID also showed strong Raman activity in both its solid and liquid form. Some drugs such as BEN and COC showed differences in Raman activity between their solid and liquid form. In this respect, BEN and COC showed stronger Raman activity in their solid form in comparison to their liquid forms (that was medium). Variation between drugs and impurities in solid and liquid forms suggested that physical properties of the substance influenced their Raman activity.

Raman Activity of Fingernails

Previous work has reported the Raman activity of key endogenous compounds such as carbohydrates, lipids, and proteins (24). Figure 3 shows the Raman spectra of endogenous compounds. Carbohydrates have been associated with the bands 1471 (CH_2 scissoring) and 808 cm^{-1} (C-C stretching) (25). The amino acids cystine and cysteine have been linked to C-S stretching vibrations that showed Raman scattering

at 623 and 643 cm^{-1} (26). These amino acids make up the disulfide bridges related to the microstructure of fingernails. Disulfide cross-linking is determinant for physical and mechanical properties of fingernail's keratin and can often be used to identify disease or nail degradation such as diabetes (27). For example, bands at 830 and 850 cm^{-1} corresponded to the presence of denatured tyrosine (amino acid) in keratin (26). This is advantageous for establishing patterns between healthy and diseased or aged fingernails. The strong C-C stretching band at 935 cm^{-1} was associated with the α-helix of the fingernail's nail plate (28). Proteins have also corresponded to S-S stretching bands at 509 – 514 cm^{-1}. CH_2 and CH_3 scissoring bands at 1447 – 1448 cm^{-1} were representative of lipids and proteins, respectively (24).

The Raman activity of fingernails was also evaluated using the aforementioned parameters. The tested fingernails (N= 20) showed strong Raman activity with 38 peaks and a signal-to-noise ratio of 56. Fingernails also demonstrated a maximum peak position of 1457 cm^{-1} and 12,000 a.u.

Raman Scattering of Fingernails

Raman activity of fingernails impacted the level of Raman scattering and this was apparent in terms of the number of bands and the Raman activity of the fingernail clippings. It is important to mention the incorporation of ORS technology and how this improved the representation of the sample's identify and composition. Traditional Raman methods incorporated a small interrogation area, whereas ORS technology ensured a larger interrogation area. The ORS technique includes a tightly focused laser beam scan over a large sample area. This provides high intensity spectra and resolution, resolving previous limitations of conventional Raman spectroscopy (29). Thus, highly complex structures can be analyzed. This ensured that all components within the fingernail clipping were collected, and a high spectral resolution maintained. Hence, Raman spectra of fingernails were highly representative of the heterogeneous components found within fingernails such as BEN, COC HCl, LEV HCl, LID HCl and PRO HCl (Figure 4).

Raman Scattering of Drugs in Spiked Nails

In the case of COC, the physical properties of the drug influenced its Raman scattering. For example, COC powder showed medium Raman scattering while COC

solution showed weak Raman scattering. However, some drugs such as LID were unaffected by physical properties and demonstrated strong Raman scattering in both powder and liquid forms. BEN was also a strong scattering regardless of the physical state. LEV and PRO showed medium scattering in both their powder and liquid forms.

Detection of Drugs in Fingernails

Spectral interpretation showed characteristic scattering bands for the chosen drug and impurities. This suggested that Raman spectra indicated key difference between the sets of spiked fingernails. The tested drug and impurity showed key bands between 400 – 1700 cm^{-1}. In this respect, Raman spectra showed key differences between the spiked fingernail sets. Fingernails spiked with COC HCl could be differentiated from BEN over the ranges 1600 – 1712 cm^{-1} (30). PRO could also be discriminated from BEN and COC over the range 1600 – 1712 cm^{-1}. For example, PRO showed key bands at 1605 (C=C stretching), 1640 (NH_2 bending) and 1695 cm^{-1} (31). Similarly, LEV could be differentiated from COC over range 460 – 1004 cm^{-1}, where COC showed key bands at 848,878 and 898 cm^{-1}, which have been associated with the C-C stretching of the tropane ring. COC also showed bands at 1278 (C-N stretching), 1453 (asymmetric CH_3 deformation), 1605 (C=C stretching) and 1712 cm^{-1} (C=O stretching) (Figure 4) (30). On the other hand, LEV showed key bands at 469 (C-S stretching), 627 (C-C bending of the benzene ring), 969 (In-plane bending related to the imidazole ring) and 1000 cm^{-1} (stretching of the mono-substituted aromatic ring) (32, 33). Furthermore, LID showed characteristic bands at 954 and 991 (C-C stretching), 1044 (C-C stretching of the aromatic ring), 1094 (C-N stretching) and 1275 cm^{-1} (C-C and C-N stretching of the aromatic ring) (30) (Table 2).

PCA scores recognized patterns in the spiked fingernail scores, which corresponded to spectral features and contributed to a high variance (Figure 5). The first three PCs contributed 70.4% of the variance amongst the spiked fingernail spectra. PC scores indicated that Raman spectroscopy and chemometrics showed the ability to differentiate fingernails spiked with COC from other drug impurities. PC1 demonstrated the highest variance among the data (42.8%) and showed scores relating to BEN, COC, LID, and PRO. PC2 showed the second highest variance

(20.8%) and accounted for BEN, LEV, and LID, and PC3 showed the third highest variance (6.8%) with scores relating to BEN. The combination of Raman spectroscopy and PCA analysis was successful in identifying and classifying the different sets of spiked fingernails where each set of spiked fingernails showed a distinct cluster (Figure 4). In this respect, no false positive was observed but false negatives were seen for the scores of BEN, LEV and PRO spectra. This could be related to two main reasons: the first being the inconsistency of distribution of drugs within fingernails and the second related to the nature of ORS in hitting multiple spots within the sample. To address this limitation in future, Raman microscopy could be used where larger areas of the sample could be measured and studied in further detail.

Conclusion

Raman spectroscopy offered a rapid and specific detection method for fingernails' endogenous constituents, COC HCl and its impurities. The results showed ORS technology resolved previous issues of conventional Raman spectroscopy such as low spectrum intensity and resolution and enhanced the Raman signal of fingernails spiked with drugs and impurities. This was ensured by a greater interrogation area and therefore advancing the overall sample's identity. Further research is needed into looking at the influence of spiking over a longer duration of time and identifying the differences between acute and chronic drug exposure.

Acknowledgements

The authors would like to thank Paul Bonser and Ian Jackson for their support of the project and for the Metrohm Mira XTR spectrometer.

References

(1) D.K. Tracy, D M. Wood, and D. Baumeister, *BMJ* 356:i6848 (2017). DOI:10.1136/bmj.i6848.

(2) United Nations Office on Drugs and Crime, (World Drug Report 2021, United Nations, New York, 2021).

(3) United Nations Office on Drugs and Crime. (World Drug Report 2019, United Nations, New York, 2019).

(4) B. Brands, B. Sproule, and J. Marshman, *Drugs & Drug Abuse*. 3rd ed: Centre for Addiction and Mental Health (1998).
(5) L.S. Goodman, L.L. Brunton, B. Chabner, and B.C. Knollmann, *Goodman & Gilman's pharmacological basis of therapeutics*. (New York: McGraw-Hill Medical, 2011).
(6) A. Poklis, R.L. Fitzgerald, K.V. Hall, and J.J. Saady, *Forensic Sci. Int.* **59**, 63–70 (1993). DOI: 10.1016/0379-0738(93)90312-X
(7) P. Saar-Reismaa, E. Erme, M. Vaher, M. Kulp, M. Kaljurand, and J. Mazina-Šinkar, *Anal. Chem.* **90**, 6253–6258 (2018). DOI: 10.1021/acs.analchem.8b00911
(8) S. Rauf, L. Zhang, A. Ali, Y. Liu, and J.H. Li., *ACS Sensors* **2**, 227–234 (2017). DOI: 10.1021/acssensors.6b00627)
(9) S. Balayssac, E. Retailleau, G. Bertrand, M.P. Escot, R. Martino, M. Malet-Martino, and V. Gilard, *Forensic Sci. Int.* **234**, 29–38 (2014). DOI: 10.1016/j.forsciint.2013.10.025.
(10) C. McKenzie, O.B. Sutcliffe, K.D. Read, P. Scullion, O. Epemolu, and D. Fletcher. *Forensic Toxicol.* **36**, 359–374 (2018). DOI: 10.1007/s11419-018-0413-1.
(11) H. Schulz, M. Baranska, R. Quilitzsch, and W. Schütze, *Analyst* **129**, 917–920, (2004). DOI: 10.1039/B408930H.
(12) C. Penido, M.T.T. Pacheco, I. K. Lednev, and L.J. Silveira, *J. Raman Spectrosc.* 47, 28–38, (2016). DOI: 10.1002/jrs.4864.
(13) S. Ewen, and G. Dent, Modern Raman Spectroscopy: A Practical Approach, (John Wiley & Sons, New York, 2005).
(14) D.A. Skoog, F.J. Holler, and S.R. Crouch, Principles of instrumental analysis. 6th ed. Cengage Learning (2006).
(15) H.H. Willard, Jr L.L. Meritt, J.J. Dean, and Jr F. A. Settle. Instrumental methods of analysis. 7th ed. New Delhi: CBS Publisher & Distributor (1988).
(16) M.J. West, M.J. Went, *Drug Test. Anal.,* **3**: 532-538 (2011). https://doi.org/10.1002/dta.217.
(17) G. Ellis, P.J. Hendra, C.M. Hodges, T. Jawhari, C.H. Jones, P. Le Barazer, and C. Passingham. *Analyst*, **114**, 1061-1066 (1989).
(18) E.A. Cutmore, and P.W. Skett, *Spectrochim Acta* A, **49**, 809-818, (1993).
(19) Scientific Working Group for the Analysis of Seized Drugs (SWGDRUG). Recommendations, version 8.0, 13 June 2019. www.swgdrug.org

(20) E.M.A. Ali, and H.G.M. Edwards. *J Raman Spectrosc*. **45**(3):253-258 (2014). https://doi.org/10.1002/jrs.

(21) H. Muhamadali, A. Watt, Y. Xu, M. Chisanga, C. Jones, D. Ellis, O. Sutcliffe, R. Goodacre, and A. Subaihi. *Front Chem*. 7: 412 (2019). https://doi.org/10.3389/fchem.2019.00412.

(22) J. Omar, B. Slowikowski, C. Guillou, F. Reniero, M. Holland, A. Boix. *J Raman Spectrosc.* **50**(1):41-51 (2019). https://doi.org/10.1002/jrs.5496.

(23) C. Eliasson and P. Matousek. *Anal. Chem.*, **79**(4):1696-1701 (2007).

(24) M. Gniadecka, O. Nielsen, D. Christensen, and H. Wulf. *J. Investig. Dermatol.* **110**(4):393-398 (1998).

(25) E. Wiercigroch, E. Szafraniec, K. Czamara, M. Pacia, K. Majzner, and K Kochan. *Biomol Spectrosc*. **185**: 317-336 (2017).

(26) A. Chiriac, D. Azoicai, A. Coroaba, F. Doroftei, D. Timpu, and A. Chiriac. Molecules. **26**(2) 280-281 (2021).

(27) P. Rich. *Dermatol Ther*. **15**(2): 107-110 (2002).

(28) B. Barry, H. Edwards, and A. Williams. *J Raman Spectrosc*. **23**(11): 641-645 (1992).

(29) A. Geravand, and S. Hashemi Nezhad. *Optik*. **178**: 83-89 (2019).

(31) I. Abdulazeez, S. Popoola, T. Saleh, and A. Al-Saadi. *Chem. Phys. Lett*. **730**: 716-622 (2019).

(32) R. Kranenburg, J. Verduin, Y. Weesepoel, M. Alewijn, M. Heerschop, and G. Koomen. *Drug Test. Anal*. **12**(10): 1404-1418 (2020).

(33) S. Shi, F. Yang, W. Yao, and Y. Xie. *Spectrosc Spect Anal*. **41**(12): 3759-3760 (2021).

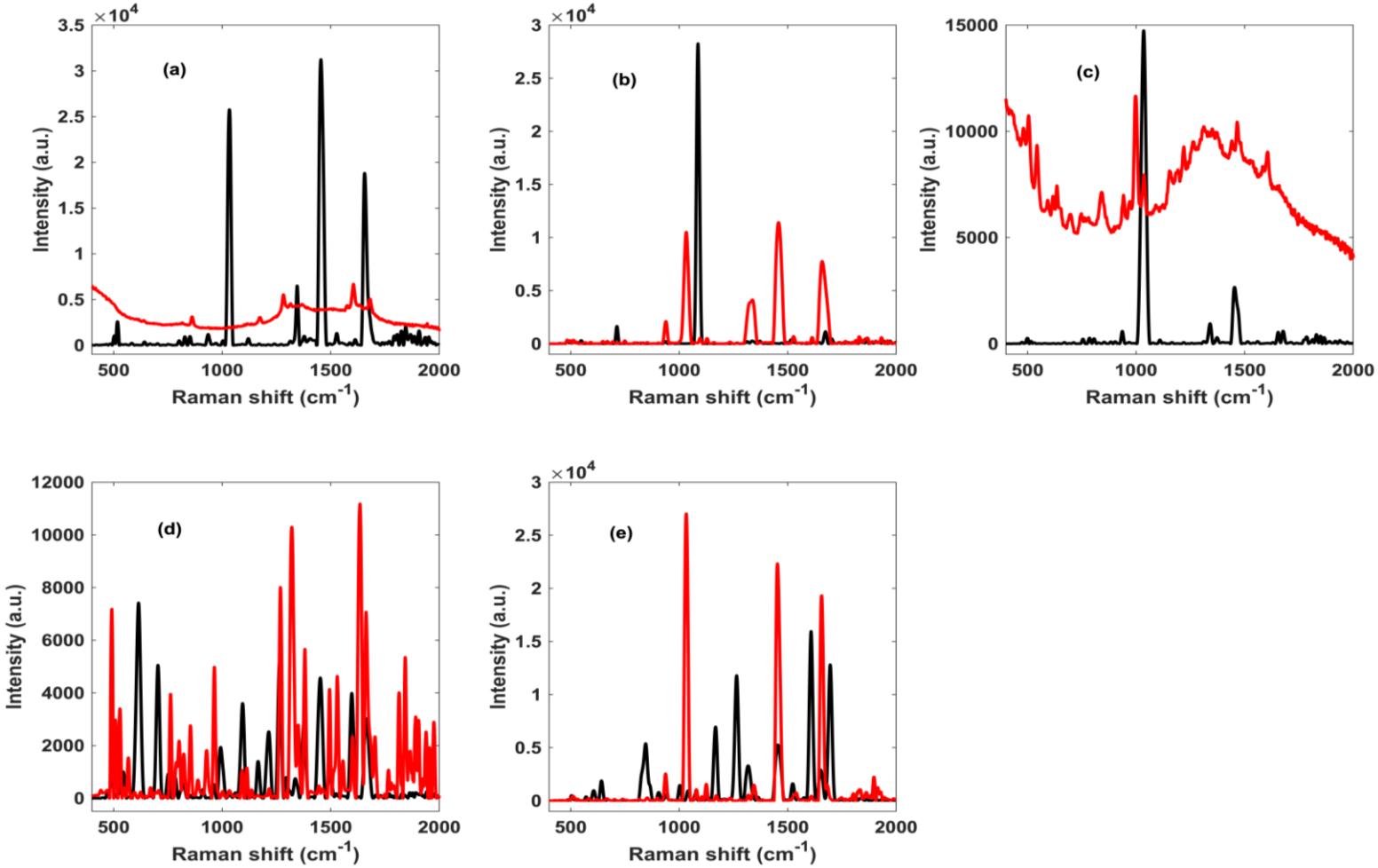

Figure 1: Raman spectra of (a) BEN (b) COC HCl (c) LEV HCl (d) LID HCl (e) PRO HCl using the handheld Metrohm Mira XTR Raman spectrometer equipped with a 785 nm laser wavelength.

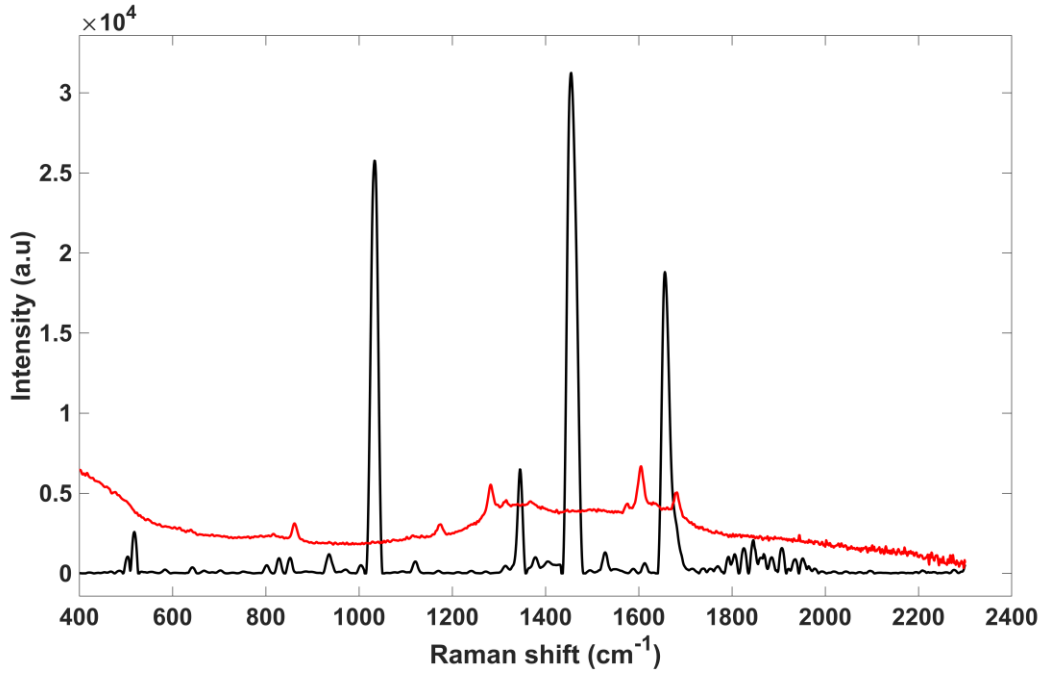

Figure 2: Raman spectra of fingernails spiked with BEN powder (black) and BEN liquid (red) forms measured using the handheld Metrohm Mira XTR Raman spectrometer equipped with 785 nm laser wavelength.

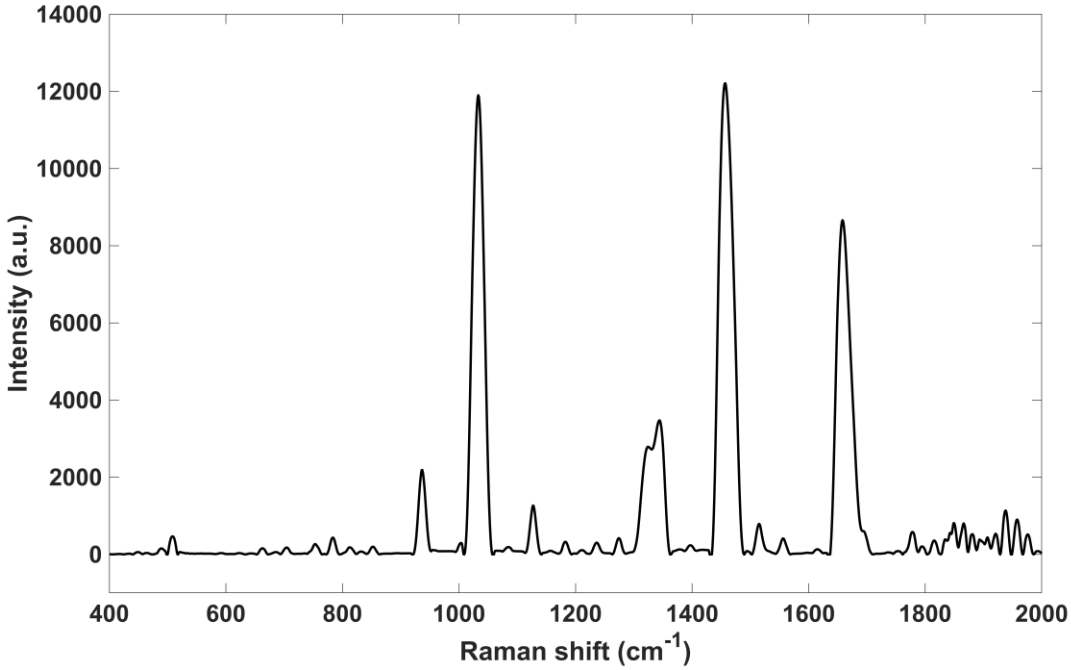

Figure 3: Raman spectra of fingernail clipping using the handheld Metrohm Mira XTR Raman spectrometer equipped with 785 nm laser wavelength.

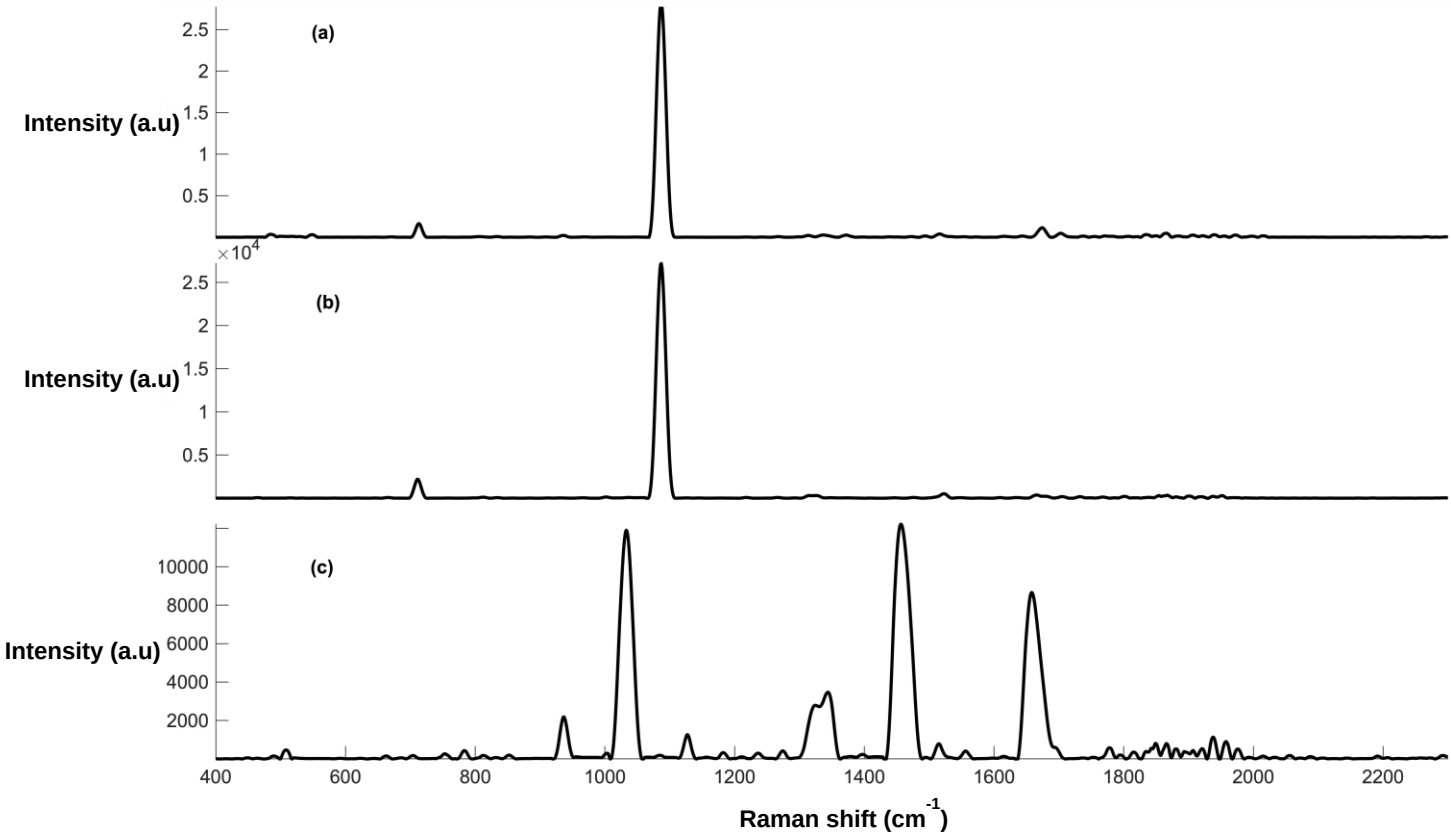

Figure 4: Raman spectra of fingernail clipping spiked with cocaine powder (a) cocaine HCl powder (b) fingernail clipping spiked with cocaine HCl powder and (c) unspiked fingernail clipping measured using the handheld Metrohm Mira XTR Raman spectrometer.

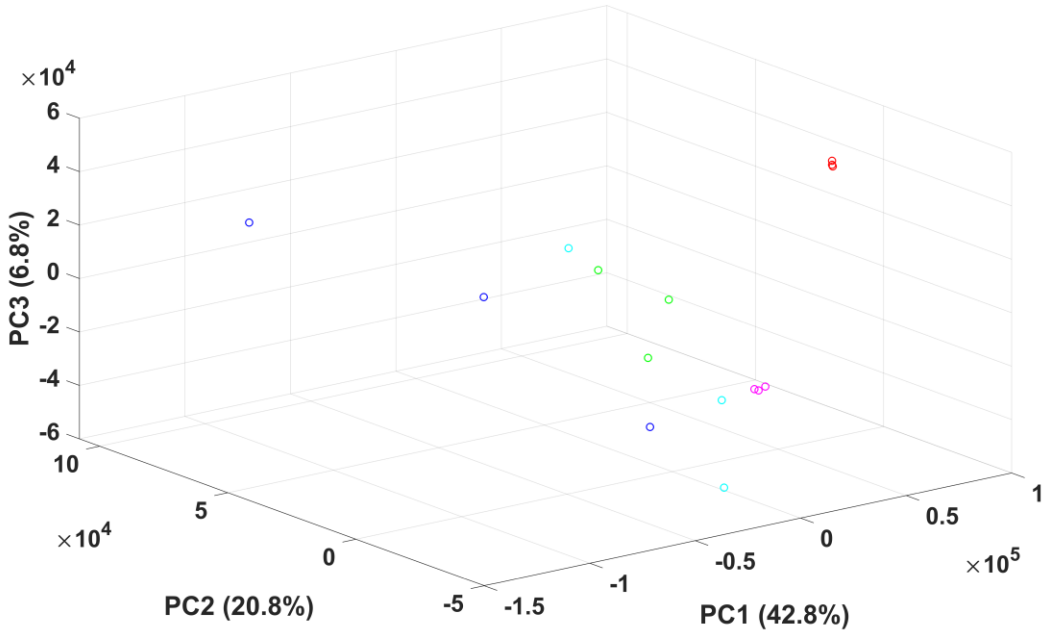

Figure 5: PCA scores plot of the Raman spectra of fingernails spiked with BEN (blue), COC HCl (red), LEV HCl (green), LID HCl (magenta), and PRO HCl (cyan).

Table I: Spectral quality of drugs and drug impurities measured using the Metrohm Mira XTR handheld Raman spectrometer equipped with a 785 nm laser wavelength.

Sample Name	*N*	*Maximum Band Position (cm^{-1})*	*Maximum Band Intensity (a.u.)*	*S/N Ratio*	*Raman Activity*
BEN powder	33	1455	31	48	S
BEN solution	28	1605	67	25	M
COC HCl powder	26	1087	28	44	M
COC HCl solution	19	1458	11	18	W
LEV HCl powder	16	1035	15	45	M
LEV HCl solution	26	996	12	35	M
LID HCl powder	29	615	74	29	S
LID HCl solution	45	1635	11	42	S
PRO HCl powder	20	1608	16	25	M
PRO HCl solution	21	1032	27	40	M

S: Strong, M: Medium, W: Weak, N: Number of peaks, S/N: signal-to-noise ratio.

The maximum band intensity unit is arbitrary units.

Absorption range of all tested drugs and impurities was 400- 2300 cm^{-1}.

Table II: Functional groups attributed to the measured drugs and impurities.

Drug or Impurity	Band Position (cm^{-1})	Corresponding Group
BEN (30)	1280	C-C/C-N/C-O stretching of aromatic ring
	1600	Stretching and bending of aromatic ring/NH_2 scissoring
	1680	C=O stretching
COC HCl (30)	848, 874 and 898	C-C stretching-tropane ring
	1004	Symmetric stretching- aromatic ring
	1278	C-N stretching
	1453	Asymmetric CH_3 deformation
	1605	C=C stretching
	1712	C=O stretching
LEV HCl (32, 33).	469	C-S stretching
	627	Benzene ring C-C bending deformation
		Imidazole ring in-plane bending
	969	Stretching of the monosubstituted aromatic ring
	1000	
LID HCl (30)	954 and 991	C-C stretching
	1044	C-C stretching – aromatic ring and C-N stretching
	1094	C-N stretching
	1275	C-C and C-N stretching - aromatic ring
	1387	C-N stretching
	1448	C-N stretching and N-H bending
	1596	Stretching and bending of aromatic ring
PRO HCl (31).	865	CH out-of-plane wagging
	1165	Aromatic CH in-plane
	1290	CN stretching
	1320	CH_2 twisting
	1520	CH bending
	1605	C=C stretching
	1640	NH_2 bending
	1695	C=O stretching